Journal of the Meteorological Society of Japan, Vol. 73, No. 4, pp. 795–809, 1995

Abrupt Seasonal Change of Large-Scale Convective Activity over the Western Pacific in the Northern Summer

By Hiroaki Ueda and Tetsuzo Yasunari

Institute of Geoscience, University of Tsukuba, Ibaraki 305, Japan

and

Ryuichi Kawamura

National Research Institute for Earth Science and Disaster Prevention, Tsukuba, Ibaraki 305, Japan

(Manuscript received 7 February 1995, in revised form 6 June 1995)

Abstract

Seasonal variations of large-scale convective activity and wind over the western Pacific are examined using Geostationary Meteorological Satellite infrared equivalent blackbody temperature (T_{BB}) and European Center for Medium range Weather Forecast (ECMWF) global analyses over a 10-year period from 1980 to 1989. In particular, this study describes an abrupt northward shift of large-scale convective activity over the western Pacific around 20°N, 150°E in late July. The enhanced convective activity is coincident with strong cyclonic circulation there which induces westerlies to the south of the cyclone and easterlies to the north of it. It is emphasized that this strong cyclonic circulation appears suddenly over the subtropical western Pacific region. Monsoon westerlies to the west of 110°E are not similary accelerated at the same time, indicating that this abrupt change is independent of the Asian monsoon system. To the north, an anticyclonic circulation is generated, which corresponds to the withdrawal of the Baiu season over Japan. Furthermore, this abrupt northward shift of large-scale convective activity is shown to be associated with tropical cyclone activity.

In the mid latitudes, geopotential height pattern between pre- and post-northward shifts of the large-scale convective activity in late July exhibit equivalent barotropic vertical structure, suggesting the Rossby-wave propagation emanating northeastward from the enhanced convective region around 20°N, 140°E (western Pacific) to as far north as 60°N, 180° (Bering Sea).

Another feature is that the seasonal increase of sea surface temperature (SST) over the key area (20°N, 150°E) precedes abrupt convective enhancement by about 20 days, exceeding 29°C in early July. It is inferred that the northeastward extension of the warm SST tongue is intimately associated with the enhanced convection in late July. This result suggests that SST warming is not a sufficient condition but certainly one important ingredient for the abrupt northward shift of convections.

1. Introduction

Ample evidence has shown that seasonal changes of various elements of the Asian monsoon are quite discontinuous in spite of a continuous seasonal variation of solar elevation. Matsumoto (1989, 1990) showed that seasonal discontinuous changes in outgoing long-wave radiation (OLR) and wind field occur almost simultaneously over wide regions in the tropics. Based upon these drastic changes, Matsumoto (1992) divided a year into eleven sub-seasons and claimed that these sub-seasons are closely associated with the advance and retreat of the monsoon. Nakazawa (1992) showed that in the OLR and wind field two active phases of intraseasonal variability (ISV) with periods of 30–60 days are both phase-locked with seasonal cycles. Enhancements are observed in both large-scale convective activity and low-level monsoon circulation fields. The first development occurs in late May and early June over the Indian Ocean which is concurrent with the climatological onset of the South India and southern Japan monsoon. A second intensification occurs in late July over the western Pacific, which is closely related to the active phase of the monsoon in middle July over the Indian Ocean. At

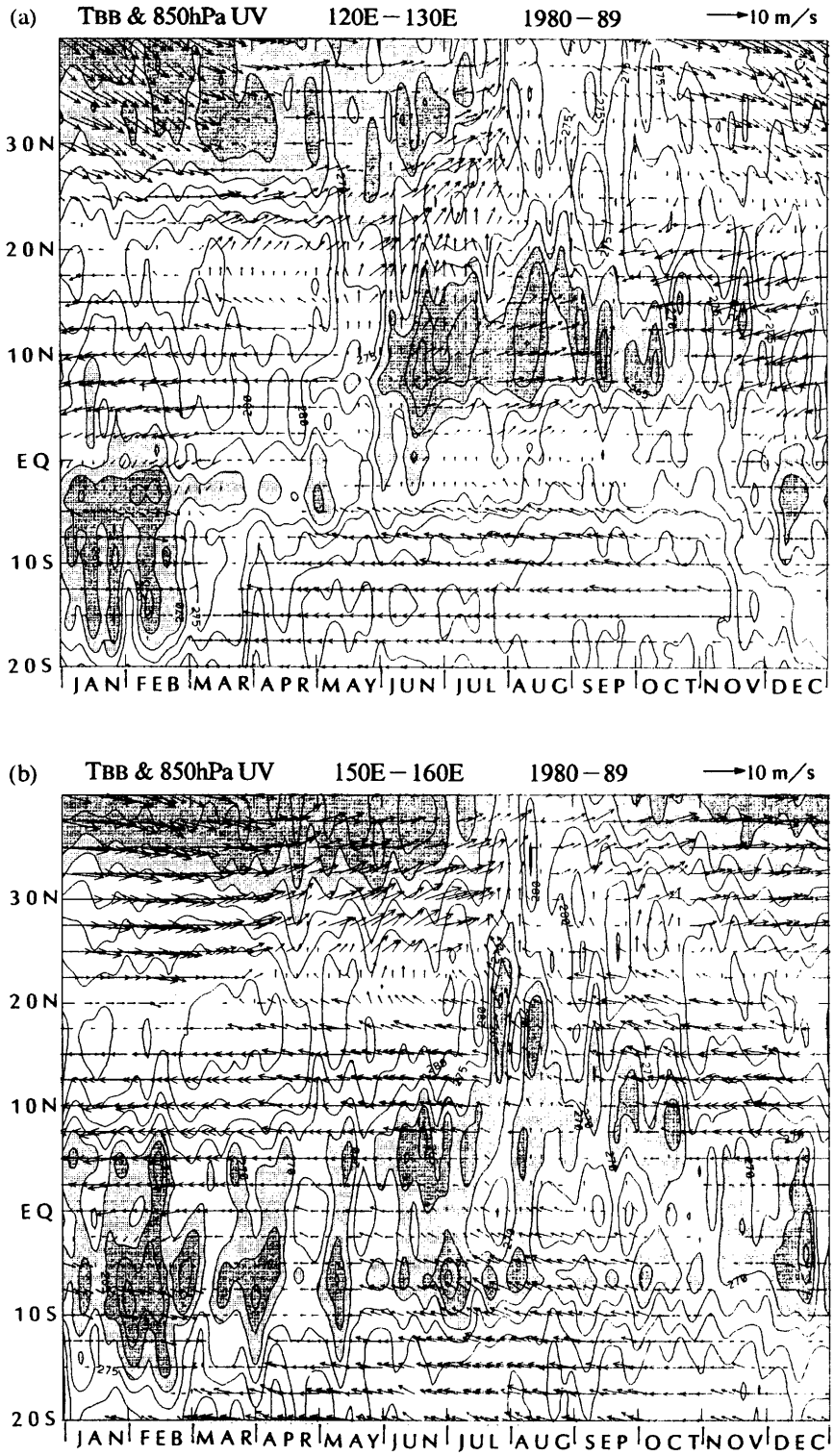

Fig. 1. Latitude-time sections of 10-year (1980–1989) averaged 5-day mean T_{BB} and 850 hPa wind averaged (a) between 120° and 130°E and (b) between 150° and 160°E. Arrows are for direction and speed of winds (unit vector 10 ms^{-1}). T_{BB} contour intervals are 5 K, and heavy shading denotes areas of less than 265 K, while light shading denotes temperatures between 265 and 270 K.

this time, (1) the monsoon westerlies "suddenly" extend over to the western Pacific as far east as 150°E, and (2) the anticyclonic circulation near Japan intensifies, resulting in the withdrawal of the Baiu (resistant frontal rain around Japan). Tanaka (1992) investigated the seasonal cycle and the onset and retreat dates of the summer monsoon in East Asia, southeast Asia and the western Pacific. Using upper clouds amount data, Tanaka showed that the rapid northward movement of cloud bands over these regions is phase-locked with intraseasonal perturbations.

Meridional heat contrast over the western Pacific is not large compared with the southeast Asian monsoon domain (T. Murakami, 1993). T. Murakami and Matsumoto (1994) indicated that the abrupt enhancement of convective activity seen in early June over the western North Pacific is caused by zonal low-level convergence due to the strong SST difference between the central and western North Pacific. They also suggested that the peak monsoon phase in middle August has a close relationship with a prominent wave packet of eastward-moving intraseasonal perturbations. Nakazawa (1992) further showed that the convective enhancement in late July has a close connection with eastward-moving ISV perturbations. He also pointed out that this enhanced convection results in the withdrawal of the Baiu season around Japan. However, the physical processes responsible for convective enhancement in late July are not well known. We use a 40-year track of tropical cyclones to examine whether tropical cyclones become major convective systems for the enhanced convection. It is also of interest to examine how SSTs in the subtropical western Pacific play a rôle in the occurrence of abrupt changes in large-scale convection.

Based on detailed observational analyses of the abrupt seasonal evolution over the western Pacific, the following questions are addressed: (1) What types of convective systems and circulation exist during the abrupt change in late July?, (2) Are there abrupt change in tropical cyclone tracks?, (3) What is the rôle of SST upon the abrupt change in convection?, and (4) What mechanisms are responsible for the withdrawal of the Baiu around Japan?

We first describe data and methods in Section 2. In Section 3, characteristic features of abrupt change in large-scale convective activity, wind fields and geopotential fields in late July are presented. In Section 4, the association of the abrupt change of convection with the track of tropical cyclones is detailed. In Section 5, the rôle of SSTs in the enhancement of convection is discussed, while Section 6 is devoted to discussions of the associated atmosphere circulation in the mid (high) latitudes. Conclusions are given in Section 7.

2. Data

Data used in this study are 1° by 1° grid mean brightness temperature (T_{BB}) obtained from the Geostationary Meteorological Satellite (GMS) compiled by the Japan Meteorological Agency (JMA) from 1980 to 1989. They are a useful index of large-scale tropical convection. The objective analysis dataset for the concurrent 10-year period analyzed by the European Center for Medium range Weather Forecast (ECMWF) is also used. Climatological 5-day mean data are then evaluated by averaging T_{BB} and global analyses over the 10-year period. In order to examine relationships with tropical convection, we also utilized 10-day mean sea surface temperature (SST) data (at a resolution of 1° latitude-longitude) over the northwestern Pacific from 110°E to 179°E between the equator and 52°N for the period January 1980 to December 1989. Charts of tropical cyclone tracks analyzed by the Typhoon Center of JMA for 40 years from 1951 to 1990 are also used in this study.

3. Seasonal changes over the western Pacific

3.1 T_{BB} and wind fields

Figure 1 shows latitude-time sections of the 10-year mean 850 hPa wind and T_{BB} fields averaged (a) between 120° and 130°E, and (b) between 150° and 160°E from January to December. The arrow indicates the horizontal wind direction and shading denotes areas of T_{BB} of less than 270 K showing most active convection in the tropics. In the upper panel of this figure, large-scale convection becomes active from December to February in the Southern Hemisphere tropics between the equator and 10°S where west winds are dominant. It is apparent that convective activity is relatively weak from March to May in both hemispheres. Suddenly, an area of active convection appears near the Philippines between 5°N and 15°N in early June and persists until October in agreement with observations by T. Murakami and Matsumoto (1994). Low-level west winds become dominant from mid-June to early September. In addition, we see the development of a low T_{BB} area around 25°N–35°N from middle May to middle July which is congruent with wet weather along the mid-latitude frontal zone (called the Baiu front).

In the lower panel, enhancement of tropical convection between 10°N and 10°S is found to occur basically on climatological intraseasonal time scales. The region of active convection abruptly shifts northward from south of 10°N up to 25°N in late July and, at the same time, the area with T_{BB} less than 270 K suddenly disappears in midlatitudes, indicating the withdrawal of the Baiu near and east of Japan. Easterlies prevailing over the western Pacific suddenly become weak and are replaced by southerlies when convection is activated

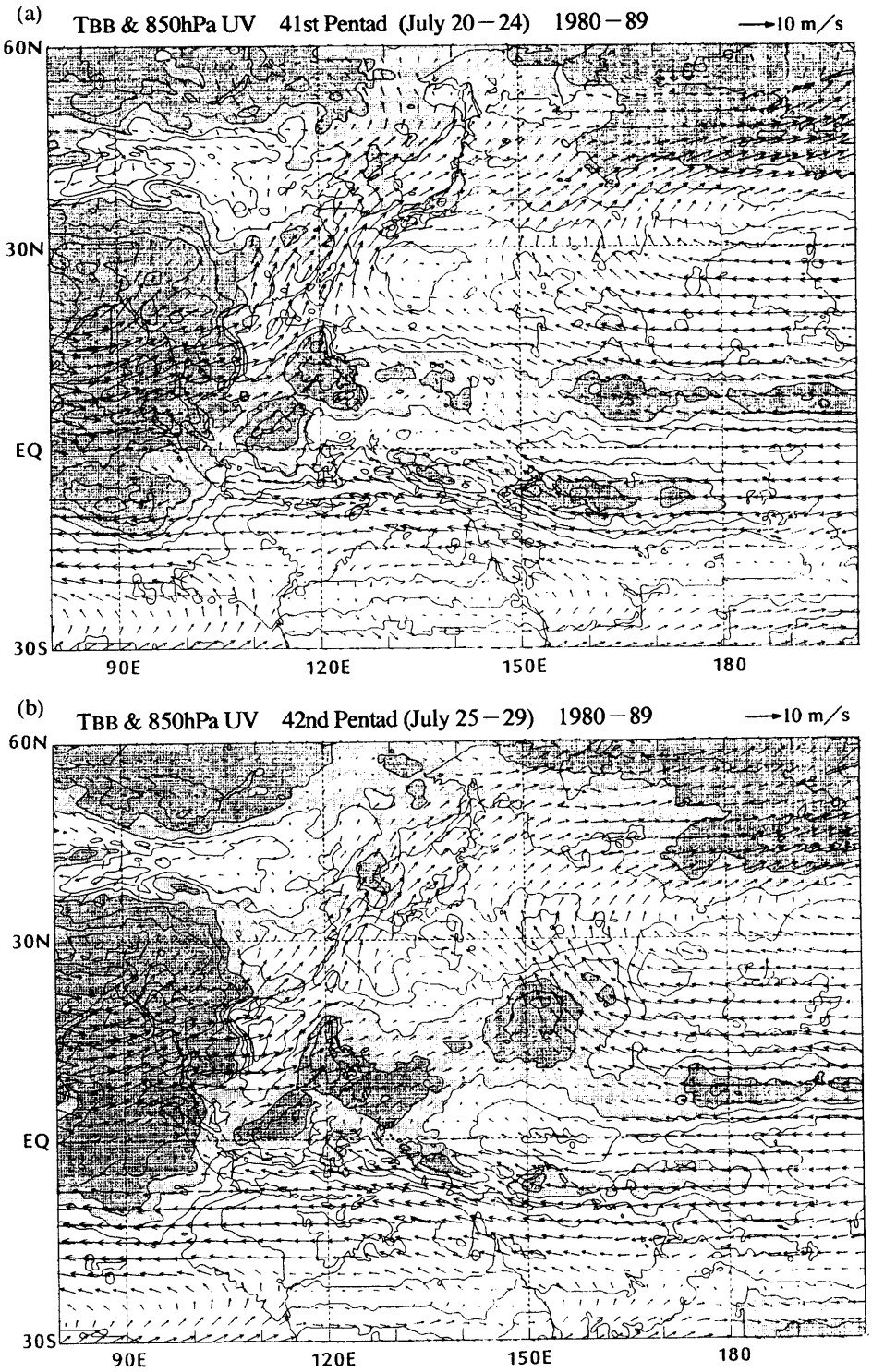

Fig. 2. Pentad mean map of 10-year averaged 850 hPa wind (unit vector 10 ms^{-1}) and T_{BB} (5 K interval) fields (a) Pentad 41 (July 20–24) and (b) Pentad 42 (July 25–29). A scale vector is shown at the upper-right of each figure. Heavy shading denotes areas with T_{BB} less than 265 K, while light shading is for areas between 265 and 270 K.

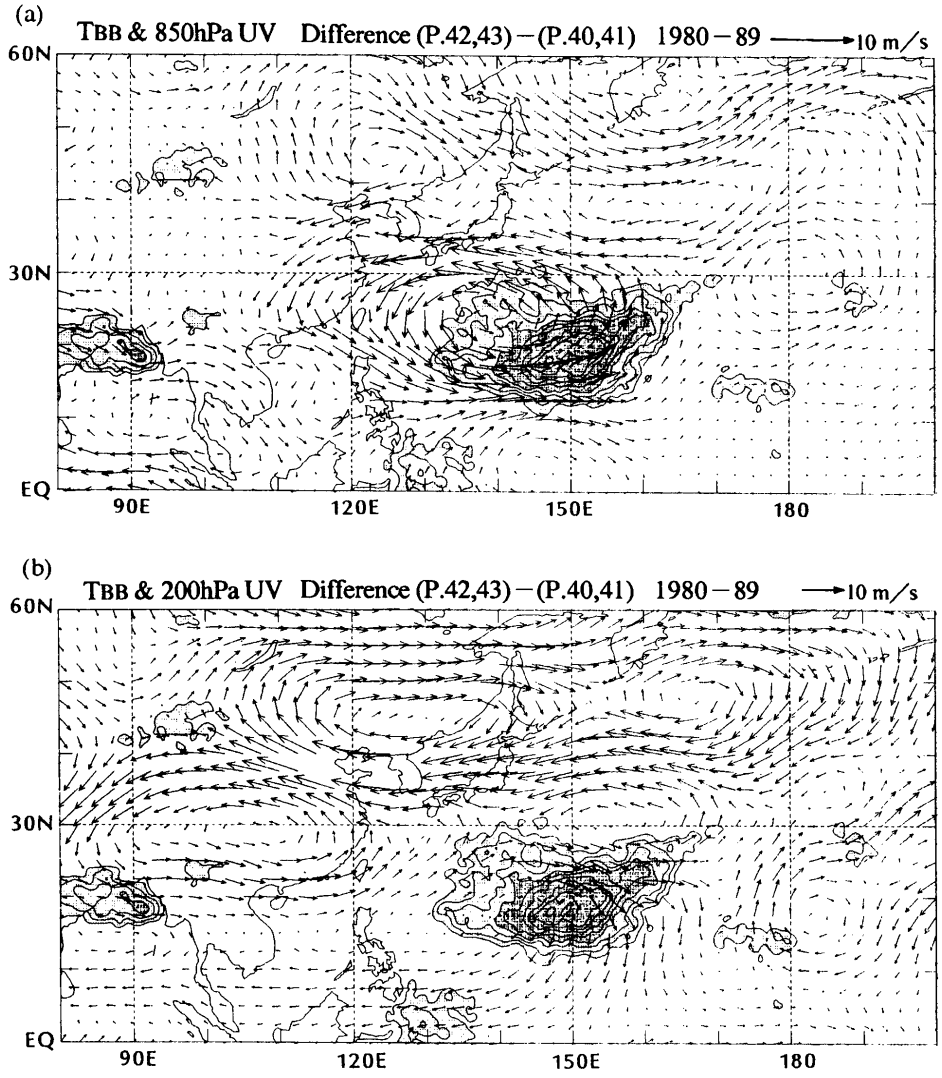

Fig. 3. Differences Pentads 42–43 minus Pentads 40–41 in T_{BB} and 850 hPa wind fields (a), and T_{BB} and 200 hPa wind fields (b). The unit wind vector is 10 ms^{-1} and the T_{BB} contour interval is 2 K. Heavy shading denotes areas of less than −8 K, while light shading is for areas between −2 and −8 K.

over the subtropical region between 15°N and 25°N from late July to middle August. After this first enhancement of convection in late July, convection suddenly suppresses with light winds during a brief period after the end of July to early August. This is followed by a second period of enhanced convection occurring again in the same region in early August. After September, active convection moves rapidly southward to 10°N and a dominant southerly component of 850 hPa winds is no longer observed over the subtropical western Pacific.

In order to examine the spatial structure of the abrupt change in late July, the horizontal distribution of the 5-day mean 850 hPa wind and T_{BB} is shown in Fig. 2. A low-T_{BB} area of less than 260 K is evident over the Bay of Bengal and the Indo. china Peninsula where low level monsoon westerlies are dominant; we can also find a low-T_{BB} area to the north of 45°N. These low values are a reflection of the cold surface not the active convection. Prior to the abrupt change at Pentad 41: July 20–24 (upper panel), the intertropical convergence zone (ITCZ) is located along 5°–10°N over the tropical western Pacific. Also evident is the low T_{BB} over Japan and Korea along the Baiu front. Furthermore, the T_{BB} is less than 260 K over the maritime continent, (*i.e.*, the Philippine Islands, Borneo, New Guinea and other small neighboring islands). In this vicinity, convection is active during day time (M. Murakami, 1983; Nitta and Sekine, 1994). As for the wind field, westerlies prevailing over the Bay of Bengal and Indo. china Peninsula turn to southwesterlies while approaching the northern Philippine Islands, eventually reaching the Korean Peninsula

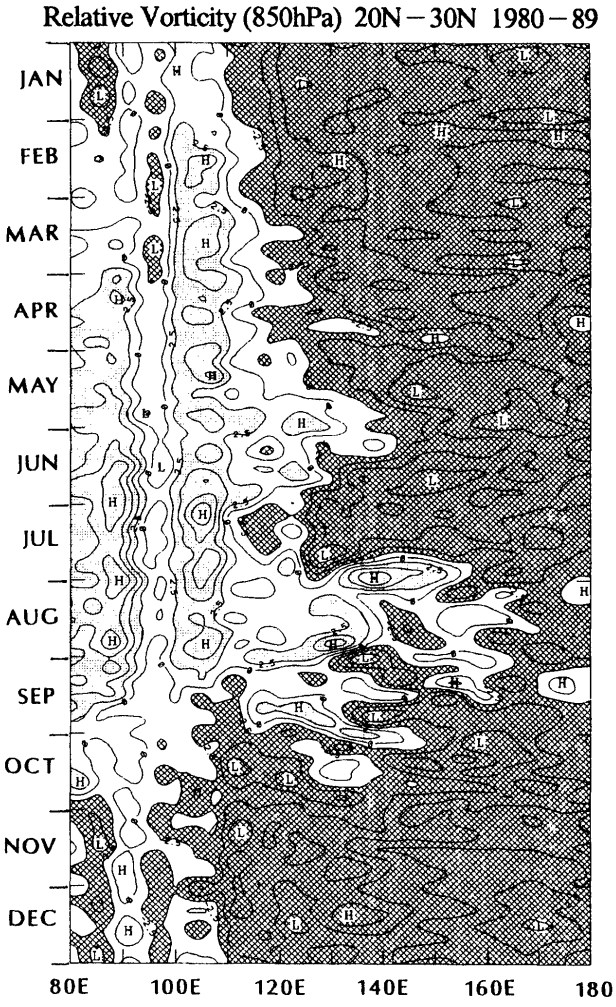

Fig. 4. Time-longitude section of 850 hPa relative vorticity averaged between 20° and 30°N with contour intervals of 2.5 s^{-1}. Light shading indicates region of greater than 2.5 s^{-1}, and heavy shading indicating regions less than −2.5 s^{-1}.

and Japan. By contrast, easterlies dominate over the tropical central and western Pacific east of 150°E and divide into two branches, one branch is directed toward the northern Philippines, the other branch is directed northward along about 150°E. The former branch merges with monsoon southwesterlies near Taiwan. In the Southern Hemisphere, easterlies are predominant between the equator and 20°S.

Figure 2b (at Pentad 42: July 25–29) depicts features during the abrupt change. One notes drastic changes in T_{BB} and wind occurring over the tropical western Pacific. The T_{BB} area of less than 260 K around 20°N, 150°E clearly indicates active convection. Another intriguing feature of Fig. 2b is that T_{BB} areas of less than 270 K disappear around Japan in a manner closely related with the withdrawal of the Baiu season. In the wind field, low-level westerlies extend eastward to the active convective region around 150°E, while low-level easterlies retreat to about 150°E. Thus westerlies converge with easterlies near 20°N, 150°E, and the resultant winds become southerly. Southerly winds further change direction to southeasterly and reach south of Japan.

Figure 3 shows the differences in T_{BB} and wind between Pentads 40–41 and 42–43. The top panel clearly shows that lower T_{BB} (*i.e.*, enhanced convection) is located over the western North Pacific with its center around 20°N, 150°E. Enhanced convective activity corresponds with an anomalous cyclonic circulation at 850 hPa with westerlies to the south of the cyclone and easterlies to the north of it. North of the easterlies, an anticyclonic circulation is generated, which corresponds to the withdrawal of the Baiu around Japan. Differences in T_{BB} and 200 hPa winds, (Fig. 3, bottom) reveal a relatively weak anticyclonic circulation anomaly around the lower T_{BB} area. Features over the active convective area suggests a baroclinic vertical structure with convergence in the lower troposphere and divergence in the upper troposphere. Also of interest is the presence of a large anticyclonic circulation anomaly extending from 100°E to the dateline along 45°N.

The zonal scale of the abrupt change in late July is examined by constructing a longitude-time cross section of 850 hPa relative vorticity averaged between 20°N and 30°N (Fig. 4). In general, positive (negative) vorticity tends to be distributed to the west of 110°E (to the east of 140°E), which corresponds to the Indian monsoon circulation (North Pacific high circulation). Occasional eastward extensions of positive relative vorticity are observed from late May to middle June, and between late July and late September. Of particular interest is a positive vorticity area appearing over the western Pacific in late July, which is consistent with the abrupt northward shift of large-scale convective activity. At this time, the zonal scale of positive vorticity over the western Pacific is approximately 50 degrees of longitude from 110° to 160°E.

3.2 Geopotential height fields

Figure 5 shows 1000 hPa geopotential heights at Pentads 41 (upper panel) and Pentad 42 (lower panel). At Pentad 41, the main axis of the subtropical ridge extends close to south of Japan around 25°N and a trough extends from the west and covers East Asia and Southeast Asia. After this period, drastic changes occur over and to the east of Japan, as shown in Fig. 5b. The monsoon trough in the western Pacific shifts northward to 20°N and extends eastward to about 150°E, which is congruent with the northward shift of tropical convection. The western edge of the subtropical ridge moves north-

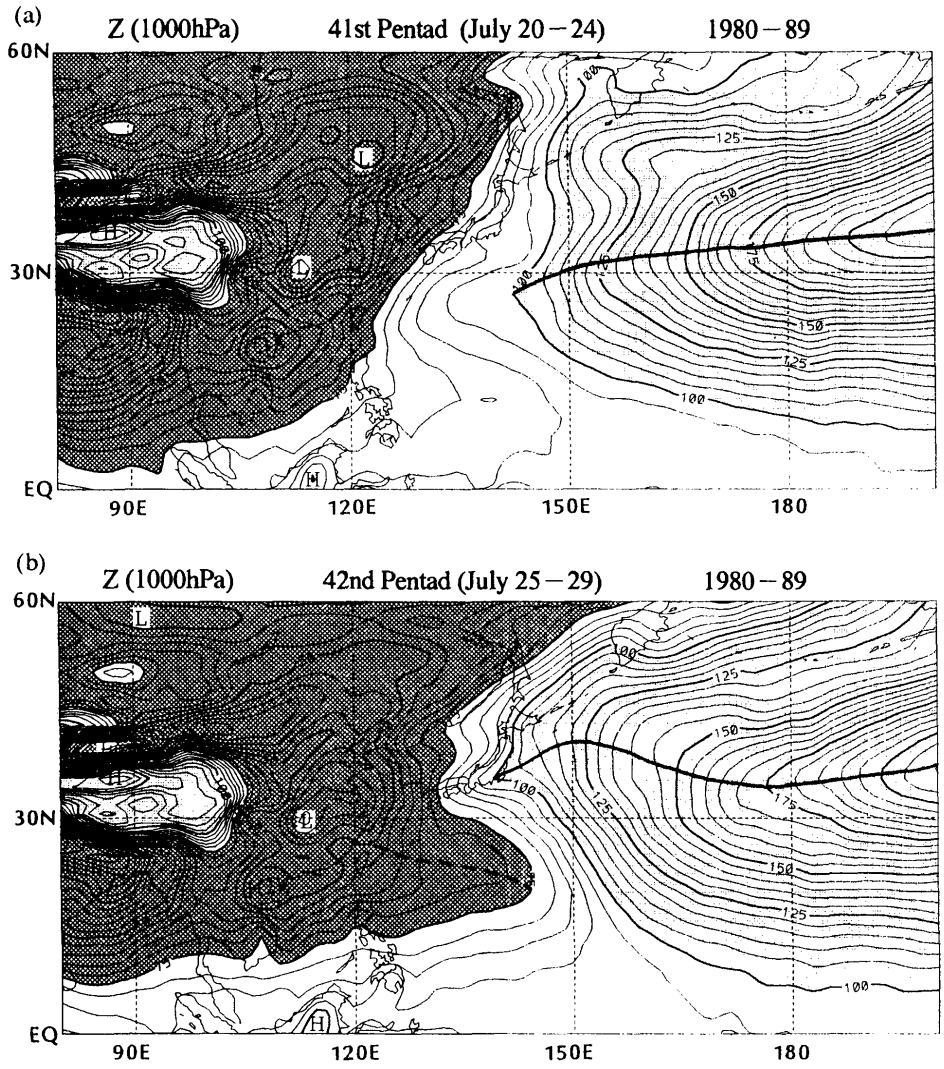

Fig. 5. Pentad mean maps of 10-year averaged geopotential height at 1000 hPa (a) Pentad 41 (July 20–24) and (b) Pentad 42 (July 25–29). The contour intervals are 5 gpm. Light shading indicates region of greater than 100 gpm, while heavy shading is for region less than 75 gpm.

ward and dominates over Japan by Pentad 42, indicating the commencement of the dry summer season in Japan. These features in late July are consistent with Nakazawa (1992), although there is a slight difference with respect to the timing of the abrupt change between his results and ours, because we define the date of abrupt change as the 42nd pentad (July 25–July 29). However, his results are based on a 10-day interval of daily mean and he considered the drastic change to occur at July 30. The average date of withdrawal of the Baiu season around Japan occurs before July 30 and is the reason why it is probable that the abrupt change can be found at Pentad 42. Furthermore, the vertical structure of the geopotential height field is not discussed by Nakazawa (1992); we further investigate this structure in the next subsection.

Differences in geopotential height between Pentad 40–41 and 42–43 are examined at various vertical levels. At 1000 hPa (Fig. 6a), marked negative height anomalies are found in the region of 20°N–30°N, 130°E–140°E, whereas positive anomalies are located from northern China to east of Japan. Negative anomalies are also observed near the Aleutian islands. 500 hPa geopotential heights (Fig. 6b) exhibit negative anomalies at nearly the same locations as those in the 1000 hPa height field with zonally elongated positive anomalies over the middle latitude region around 40°–50°N. Negative height anomalies are seen again north of 55°N. At 200 hPa (Fig. 6c), one should not overlook the appearance of negative anomalies over the subtropical western North Pacific around 20°N, 140°E–150°E. Over the mid-latitude region from 40°N to 50°N, remarkable positive height anomalies extend zonally from the northern China-North Pacific region. Anomaly pat-

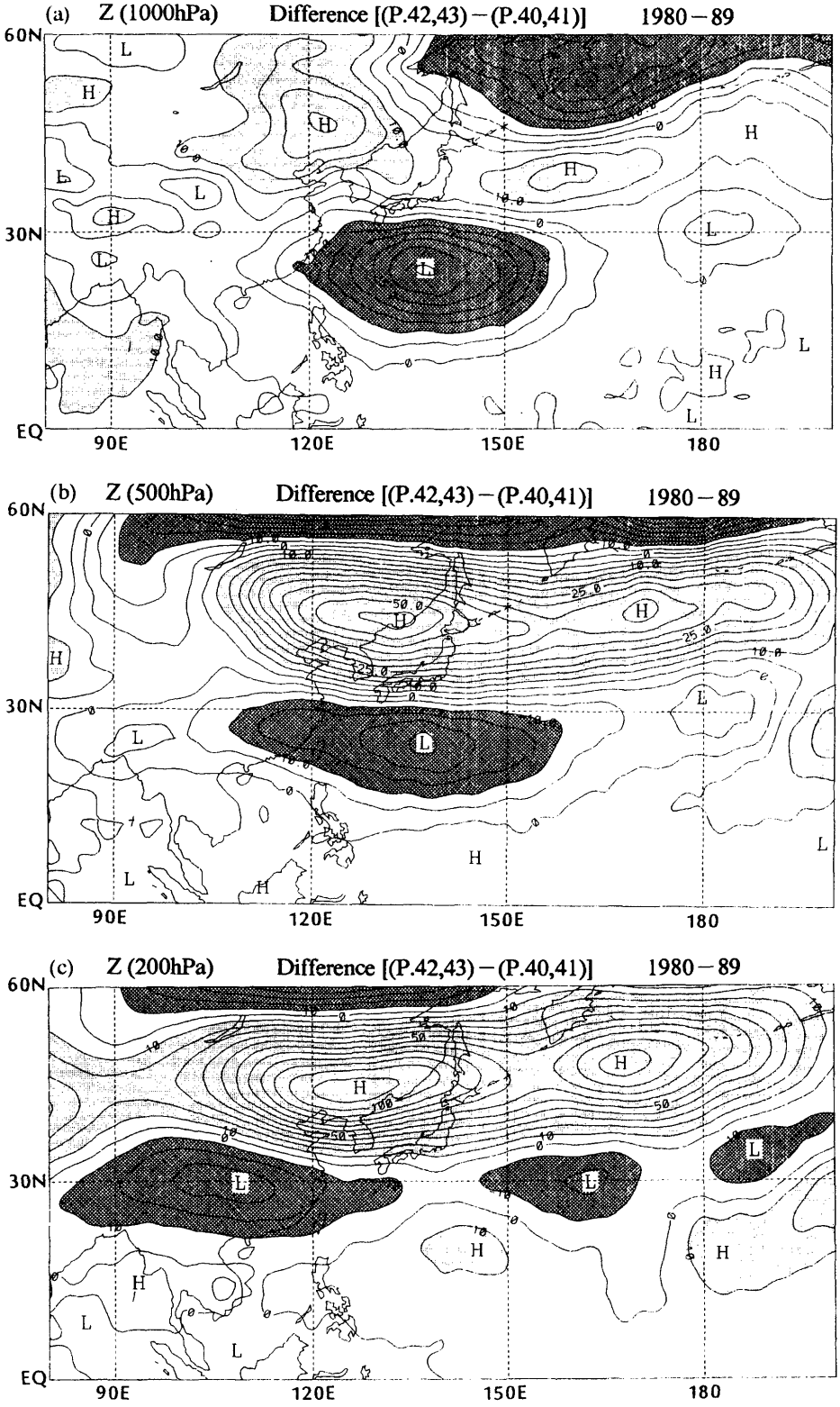

Fig. 6. Differences in geopotential height between Pentads 42–43 minus Pentads 40–41, computed at (a) 1000 hPa, (b) 500 hPa and (c) 200 hPa, respectively. The contour interval is (a), (b) 5 gpm and (c) 10 gpm. Light shading is for greater than 10 gpm, while heavy shading for less than −10 gpm.

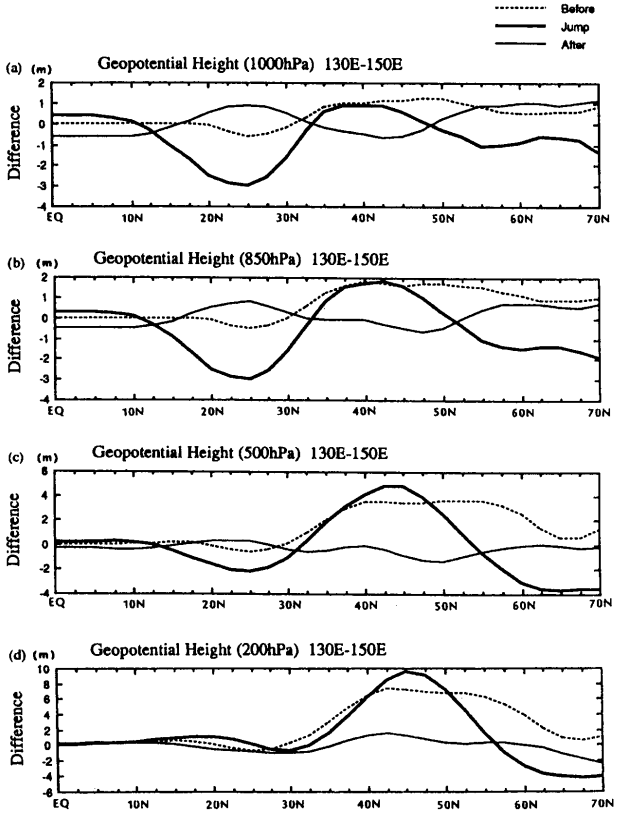

Fig. 7. Meridional profiles of geopotential height averaged between 130° and 150°E at (a) 1000 hPa, (b) 850 hPa, (c) 500 hPa and (d) 200 hPa, respectively. The broken, bold and solid line indicates differences between Pentads 39–40 minus 37–38, between Pentads 42–43 minus 40–41, between Pentads 45–46 minus 43–44, respectively.

terns over the active convective area indicate a baroclinic vertical structure with an anomalous cyclone in the lower troposphere (Fig. 6a), as contrasted with an anomalous anticyclone in the upper troposphere (Fig. 6c). On the other hand, over the middle latitude region of 35°N–55°N, geopotential height anomalies exhibit barotropic structure in the vertical.

In order to examine time changes of geopotential height between three phases before, during, and after the abrupt jump of the active convection in late July, three meridional time sections at each geopotential height level averaged between 130°E and 150°E were constructed. In Fig. 7, broken, bold, and solid lines represent changes in geopotential heights for the three phases; Pentads 39–40 minus Pentads 37–38, Pentads 42–43 minus Pentads 40–41, and Pentads 45–46 minus Pentads 43–44, respectively.

At 1000 hPa (Fig. 7a), the bold line reveals a significant meridional variation with two minima at

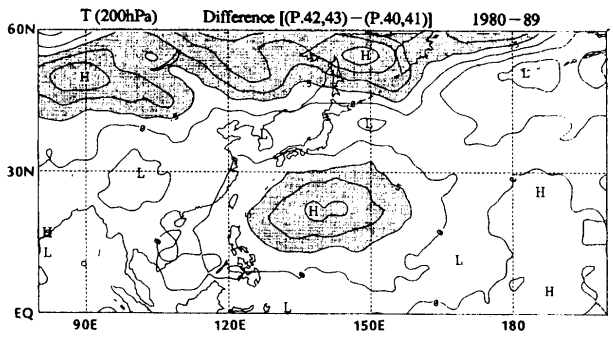

Fig. 8. Difference in 200 hPa temperature between Pentads 42–43 minus Pentads 40–41 with a contour interval of 0.5 K. The shaded areas denote a positive temperature difference greater than 0.5 K.

25°N and 55°N and one maximum at 40°N. The minimum value at 25°N corresponds to active convection in late July and the maximum value around 40°N is considered as a result of the Rossby response by enhanced convection around 25°N. It is interesting to note that this pattern can not be clearly recognized at phases before and after the abrupt change (the broken and solid line), except for around 40°N–50°N with broken line ("Before"). Before the abrupt change, an increase of geopotential height north of 35°N is thought to be a continuous maturing process of the summer season in midlatitudes. During the jump period, the increase of geopotential height north of 35°N is slightly greater than at other periods. In addition, a decrease of geopotential height north of 55°N at the jump period is evident compared with other periods of "Before" and "After" which may be caused by Rossby wave response. Similar patterns are also found at 850 hPa (Fig. 7b), 500 hPa (Fig. 7c) and 200 hPa (Fig. 7d), each showing positive (negative) anomalies over mid-latitudes around 45°N (north of 60°N and near 25°–30°N of enhanced convection). This stands in sharp contrast with geopotential patterns before and after the abrupt change. In this manner, the abrupt change in late July is extremely peculiar when compared to other phases from June to August.

Relations between atmospheric temperature and convection are shown in Fig. 8, depicting differences in 200 hPa temperature for Pentads 42–43 minus Pentads 40–41. Shading denotes warming greater than 0.5°C. A warming maximum of 1.5°C can be found over the subtropical western Pacific near 25°N, 140°E, which is separated from a midlatitude warming region north of 40°N. Of course, warming over the subtropical western Pacific corresponds to an atmospheric response to convection, as shown in Fig. 3. However, the heating rate of 1.5°C per two pentads is not particularly large and, ac-

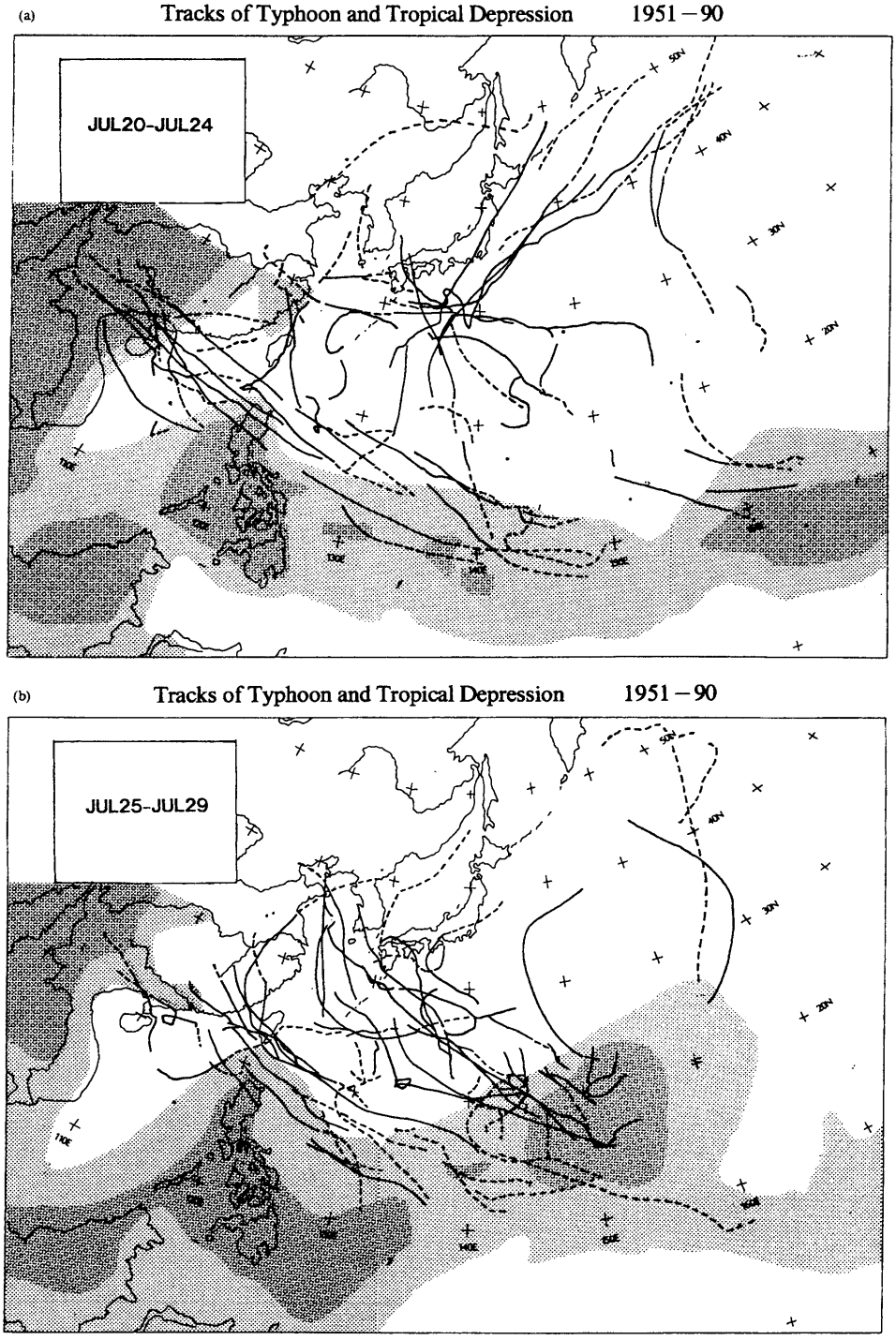

Fig. 9. Tracks of typhoons and tropical depressions over the period from 1951 to 1990 at (a) Pentad 41 (July 20–24), and (b) Pentad 42 (July 25–29). The solid (broken) lines indicate typhoons (tropical depressions). Also shown is 10-year averaged pentad mean T_{BB} with heavy shading for less than 265 K, and light shading for 265 to 270 K.

cordingly, the 200 hPa anticyclone in Figs. 3b, and 6c is not very significant, either.

4. Tropical cyclone activity in late July

As pointed out by Kawamura *et al.* (1994), tropical cyclone activity is likely to be closely associated with the abrupt northward shift of large-scale convective activity in late July. Nakazawa (1992) examined tropical cyclones in July using longitude-time cross sections of tracks of tropical cyclones averaged between the equator and 15°N, as well as between 15°N and 30°N for the period 1871 to 1982, and con-

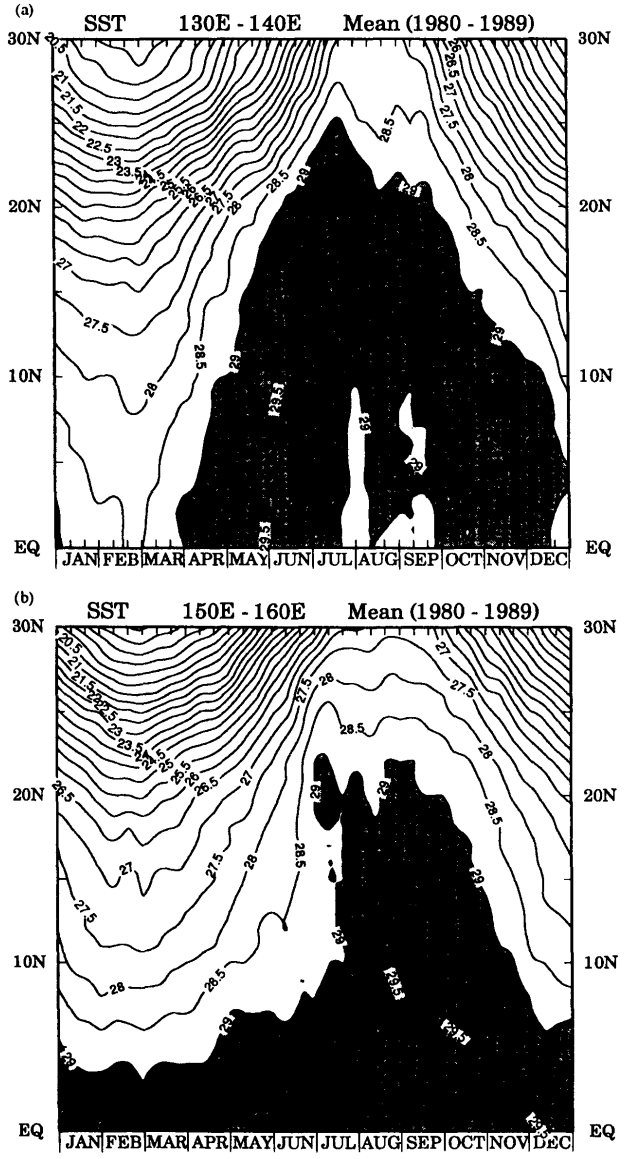

Fig. 10. Latitude-time sections of 10-year averaged 10-day mean SST averaged (a) between 130°–140°E and (b) between 150°–160°E. The contour interval is 0.5°C. Shading denotes areas of greater than 29°C.

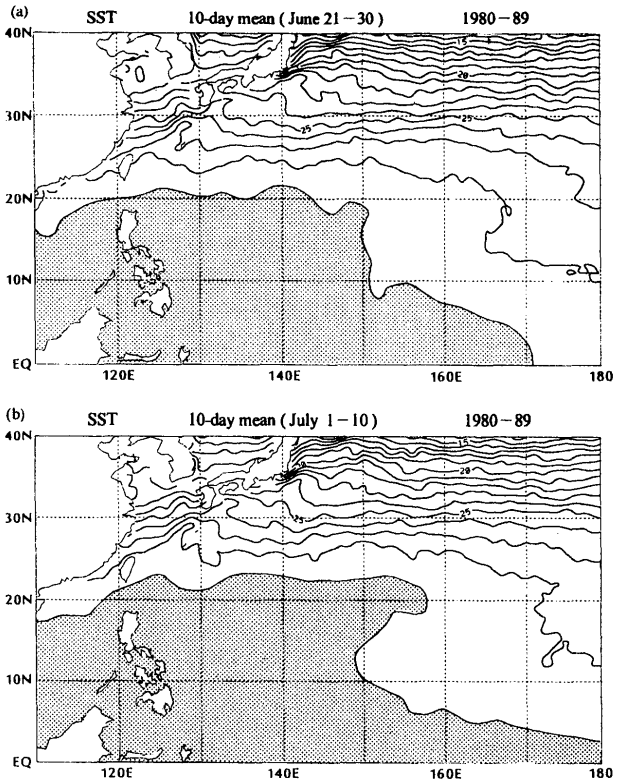

Fig. 11. 10-day mean map of 10-year averaged SST (a) June 21–30 and (b) July 1–10. The contour interval is 0.5°C. The shaded areas are for SST greater than 29°C.

cluded that more tropical cyclones are observed in July compared with June and August. We further examine the relationships between abrupt change of the convective activity and the tropical cyclone in late July (Pentads 41, 42) utilizing cyclone tracks from 1951 to 1990 produced by the JMA.

Figure 9 shows tracks of tropical cyclones for (a) Pentad 41, and (b) Pentad 42, which correspond to phases before and during the abrupt change in T_{BB} fields, respectively. In Fig. 9a, tropical cyclone tracks seem to be divided into two groups: one westward-moving group from the western Pacific around 5°N–15°N, 140°E–150°E to the southern part of China and one northward-moving group toward the Kuroshio region south of Japan. A typhoon free area is noted around 15°–20°N from 140°E to 150°E. Tracks of tropical cyclones at the abrupt change (Fig. 9b) clearly indicate more frequent development of tropical cyclones over the western Pacific around 15°N–25°N, 140°E–150°E. In contrast, no tropical cyclones formed to the east of 155°E. Enhancement of large-scale convective activity around 20°N, 150°E at Pentad 42 as derived from T_{BB} corresponds with a remarkable increase in the frequency of tropical cyclones over the same region. Thus, long-term tropical cyclone data (40 years) confirm that the abrupt change in convective activity at Pentad 42 can be regarded as significant, rather than an artifact due to short sampling of ECMWF and T_{BB} data.

5. Seasonal change of SST

Sea surface temperature (SST) must be one of the important physical factors for the determination of convective activity. In this section we investigate characteristic features of seasonal evolutions of SST over the western Pacific, in particular dur-

ing July. Figure 10 shows latitude-time sections of SST averaged over (a) 130° through 140°E, and (b) 150° through 160°E. Gadgil *et al.* (1984) showed that convection is abruptly enhanced when SST rises more than 28 to 29°C over the tropical ocean. Seasonal changes of SST along 130°–140°E (Fig. 10a) during July are both continuous and slow. Here, SSTs at 20°N rise gradually from March to middle July and the warmest conditions (in excess of 29°C) persist until the end of September. On the other hand, seasonal evolution of SST around the corresponding region of enhanced convection (Fig. 10b) is quite different from spring to summer . SSTs higher than 29°C suddenly appear between 18°N and 22°N in early July. The increase in SST leads to enhanced convection over the same region about 20 days later. In contrast, SST remains less than 29°C to the south between 8°N and 18°N until the end of July. Moreover, SST higher than 29°C once again occurs at almost the same latitudes in early to middle August, followed by a decrease in middle to late August from 18 to 21°N. It is noteworthy that an SST rise to more than 29°C precedes active convection by about 20 days.

Figure 11 represents the spatial distribution of 10-day mean climatological SST for (a) late June and (b) early July. At the end of June (Fig. 11a), the area of SST exceeding 29°C is found to extend northward up to 20°N and eastward of 150°E. In early July, the area with SST higher than 29°C further extends northward to 22°N, while a somewhat peculiar eastward extension of SST higher than 29°C occurs from 150°E to 158°E along about 20°N.

Here arises a question: why does SST increase over the above region in early July? Hsiung and Newell (1983) showed good correlation between SST and incoming solar radiation over the Pacific on interannual time scales. However, interactions in the seasonal evolution is not clearly understood. From the figure of 5-day mean 850 hPa wind and T_{BB} at Pentad 37: June 30–July 4 (not shown), which corresponds to the period of abrupt SST warming in early July, the ITCZ is located along the equator and 10°N over the tropical Pacific, while active convection can not be found north of the ITCZ to 30°N over the subtropical western Pacific. As for winds, easterlies prevail over the tropical western Pacific to the east of 130°E and direct toward southward of Japan, merging with monsoon westerlies. Confluent winds further change direction to southwesterlies over the subtropical western Pacific around 30°N. Of particular interest in this figure is that very weak winds and a high T_{BB} of more than 285 K can be seen over the region around 20°N between 140°–150°E, which is coincident with the abrupt SST warming region in early July. It is speculated that strong insolation and decreases of both turbulent mixing and evaporative cooling due to inactive convection and weak winds may lead to SST warming. On the other hand, it is possible that strong easterlies dominate south of the abrupt-change region of SST between 10°–18°N (Fig. 11b), which induce turbulent mixing of underlying water which may suppress SST warming. However, further studies are needed to clarify how SST in the subtropical western Pacific is related to the atmosphere on seasonal time scales.

Recall that the warm SST tongue around 20°N, 155°E in early July coincides closely with enhanced convection during late July, *i.e.*, about 20 days later. These results suggest that SST warming is not a sufficient condition but rather an important condition for convective activity. At present, however, whether SST increases are really responsible for the enhancement of the convection after 20 days is not clear.

6. Response of extratropical circulation

This study indicates that the abrupt northward shift of large-scale tropical convective activity has a strong influence on the extratropical atmosphere. Nakazawa (1992), based on climatological OLR and 1000 hPa geopotential height, discussed relationships between withdrawal of Baiu near Japan and tropical convection and concluded that northward extension of the subtropical ridge in late July is intimately associated with the northward shift of large-scale tropical convective activity in the western Pacific. To clarify the vertical structure and poleward propagation of stationary Rossby waves, differences in both 1000 hPa and 500 hPa geopotential heights between Pentads 42–43 and 40–41 are presented in Fig. 12. The 1000 hPa geopotential difference pattern (Fig. 12a) shows negative anomalies over the tropical western Pacific, and positive anomalies covering the midlatitudes, northeast China, east of Japan, and prominent negative anomalies appearing over the Aleutian Islands and the northwest Pacific. One notes similar anomaly patterns at the 500 hPa geopotential difference field (Fig. 12b), thus implying an equivalent barotropic structure in wave trains. These results indicate the possibility that a stationary Rossby wave is forced and propagates from the enhanced convective region to the extratropical regions, which may bring about withdrawal of the Baiu and commencement of summer season near Japan.

Existence of Rossby wave propagation generated by the heat source located in the tropical western Pacific, which is associated with ISV, has been suggested by Nitta (1987). He showed that high pressure anomalies over East Asia and the northwestern Pacific can be understood as a result of frequent occurrences of Rossby wave propagations generated over the maritime continent during anomalous warm SST summers. However, our results are different

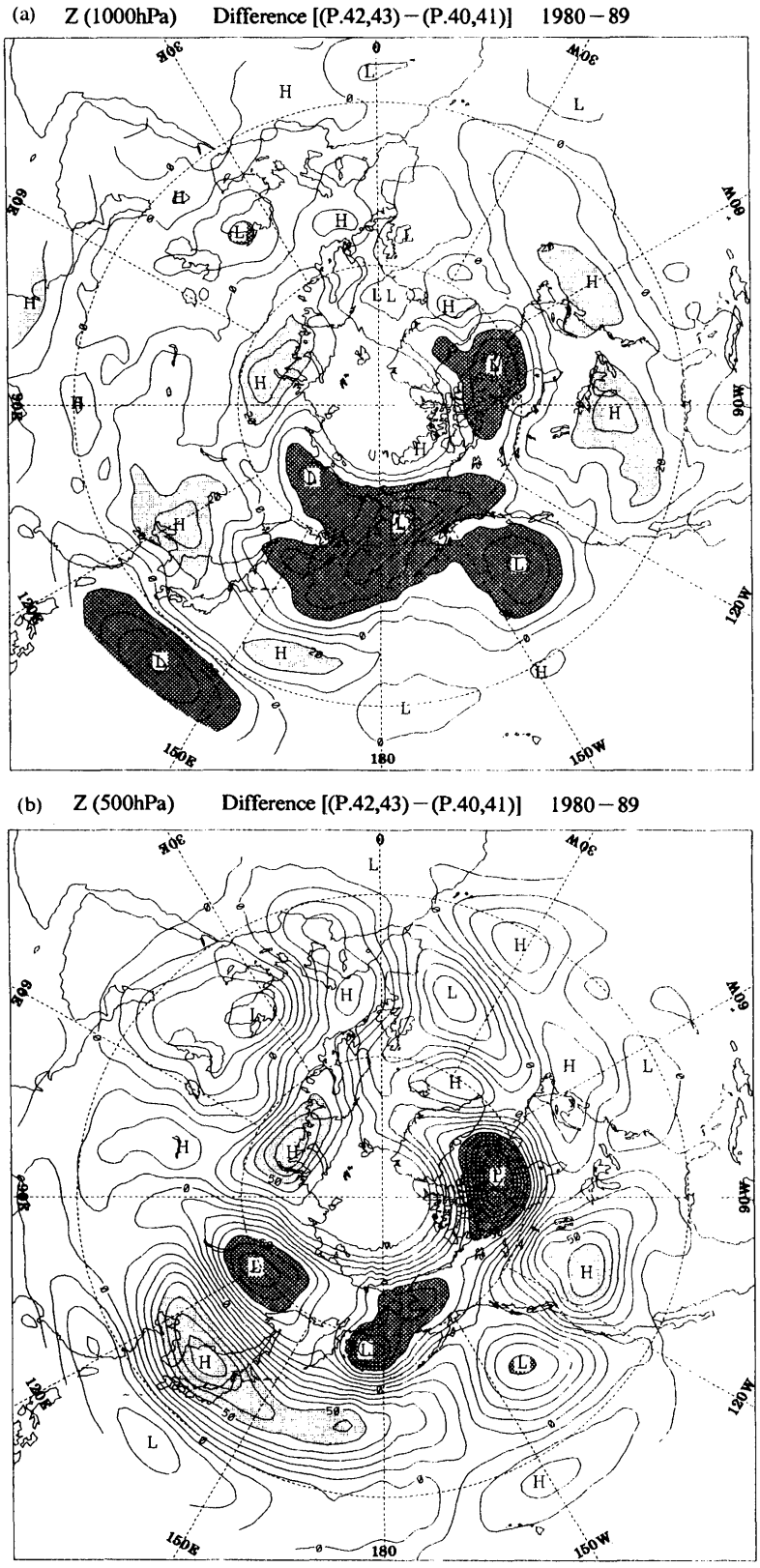

Fig. 12. Differences in the geopotential height for Pentads 42–43 minus Pentads 40–41 at (a) 1000 hPa and (b) 500 hPa. The contour interval is 10 gpm. Light shading denotes regions with greater than (a) 20 gpm and (b) 50 gpm, while heavy shading is for region less than (a) −20 gpm and (b) −50 gpm.

from his in terms of the time scale and the place because his results are based on a warm SST summer season and Rossby-wave trains starting near the maritime continent. Our study reveals the signature of a Rossby wave-like propagation from around 25°N, 140°E over the subtropical western Pacific in late July which is climatologically phase locked. Kurihara and Tsuyuki (1987) also investigated relationships between development of the subtropical high around Japan and convective activity over the northwestern tropical Pacific during August 1984. By using a linear shallow water model, they examined the atmosphere response to forcing north of the Philippines, and claimed that development of the barotropic high near Japan is associated with energy dispersion from barotropic Rossby waves excited by intensified convection. Kawamura and Tian (1992) selected the singularity of fine weather in Japan and examined relationships between its maintenance or breaking mechanism and the 500 hPa geopotential field anomaly pattern. They suggested that fine weather in late July (Pentad 42) in Japan is closely associated with the Rossby wave propagation from low latitudes of the western Pacific. Their finding supports our study with respect to a climatological phase-lock feature of the Rossby wave propagation.

In conclusion, the point we would like to emphasize is that the northward shift of large-scale convective activity primarily associated with tropical cyclones in late July has an impact upon the withdrawal of the Baiu near Japan, as well as upon climatic changes over the Northern Pacific via the starting of Rossby wave propagation. It is suggested that tropical cyclones are a major rain producer and provide energy sources for possible barotropic stationary Rossby wave propagation from the subtropical western Pacific to the midlatitudes in late July. In addition, it is important that this Rossby wave propagation can be observed in the seasonal cycles at Pentad 42, which is essentially different from Nitta's result on the aspect of time scale.

7. Concluding remarks

Major findings obtained in this study are summarized as follows:

1) Climatological 10-year mean pentad values of T_{BB}, wind and geopotential fields clearly show abrupt seasonal changes occurring over the western Pacific in late July. Particularly, an abrupt northward shift of active convection is noticeable from 10°N up to 25°N.

2) Enhanced convective activity over the subtropical western Pacific during late July around 20°N, 150°E corresponds to a cyclonic circulation in the lower troposphere and an anticyclonic circulation in the upper troposphere.

3) During the abrupt change, the monsoon trough over the western Pacific in the lower troposphere extends southeastward through the active convective region near 150°E. The subtropical ridge rapidly moves northward and covers Japan, which marks the end of the Baiu rainy season there. Differences in geopotential heights associated with the abrupt change clearly exhibit a barotropic structure from the subtropical western Pacific to higher latitudes, which suggests that the Rossby wave propagation is forced by the enhanced convection to the south of Japan.

4) A dramatic change of tropical cyclone tracks is also noticed based on the 40-year cyclone data before and after the abrupt northward shift of enhanced convection activity seen in the T_{BB} field, which actually contributes to the abrupt seasonal change of large-scale convective activity.

5) Before the abrupt change in late July, we found a drastic change of SST in the region where the abrupt change occurs. In early July, a warm SST pool in excess of 29°C around 20°N extends eastward from 150°E to 158°E, which is collocated with the activated convective region in late July, with a 20-day time lag. These results indicate the importance of SST warming on the abrupt northward shift of tropical convection.

Acknowledgments

The authors are indebted to Prof. Takio Murakami of University of Hawaii whose comments greatly improved the clarity of the paper. Special thanks are due to Dr. Jun Matsumoto of University of Tokyo for stimulating discussions. They also thank Prof. Tsuyosi Nitta of the University of Tokyo for many valuable comments and Dr. Testuo Nakazawa of Meteorological Research Institute for providing them with the T_{BB} data. Computation was performed with the CRAY Y-MP2E/264 supercomputer of National Research Institute for Earth Science and Disaster Prevention.

References

Gadgil, S., P.V. Joseph and N.V. Joshi, 1984: Ocean-atmosphere coupling over monsoon regions. *Nature*, **312**, 141–143.

Hsiung, J. and Newell, R.E., 1983: The principal nonseasonal modes of variation of global sea surface temperature. *J. Phys. Oceanogr.*, **13**, 1957–1967.

Kawamura, R. and S.-F. Tian, 1992: Singularity in Japan and teleconnection patterns appearing in 500 hPa geopotential height field of the Northern Hemisphere. *Tenki*, **39**, 75–85 (in Japanese).

Kawamura, R., T. Yasunari and H. Ueda, 1994: Abrupt changes of seasonal evolution of large-scale convective activity and tropical cyclone over the western Pacific. *Report of the National Research Institute for Earth Science and Disaster Prevention*, **53**, 1–18 (in Japanese with English Abstract).

Kurihara, K. and T. Tsuyuki, 1987: Development of the barotropic high around Japan and its association

with Rossby wave-like propagations over the North Pacific: Analysis of August 1984., *J. Meteor. Soc. Japan*, **65**, 237–246.

Matsumoto, J., 1989: The seasonal changes of tropical cloud distribution as revealed from 5-day mean outgoing longwave radiation. *Bull. Dept. Geogr. Univ. Tokyo*, **21**, 19–35.

Matsumoto, J., 1990: The seasonal changes of wind fields in the global tropics. *Geogr. Rev. Japan*, (*Ser. B*), **63**, 156–178.

Matsumoto, J., 1992: The seasonal changes in Asian and Australian monsoon regions. *J. Meteor. Soc. Japan*, **70**, 257–273.

Murakami, M., 1983: Analysis of the deep convective activity over the western Pacific and Southeast Asia. Part I: Diurnal variation. *J. Meteor. Soc. Japan*, **61**, 60–77.

Murakami, T., 1993: Nature of monsoon Asia. *kagaku*, **63**, 619–625 (in Japanese).

Murakami, T. and J. Matsumoto, 1994: Summer monsoon over the Asian continent and western North Pacific. *J. Meteor. Soc. Japan*, **72**, 719–745.

Nakazawa, T., 1992: Seasonal phase lock of intraseasonal variation during the Asian summer monsoon. *J. Meteor. Soc. Japan*, **70**, 597–611.

Nitta, Ts., 1987: Convective activities in the tropical western Pacific and their impact on the Northern Hemisphere summer circulation. *J. Meteor. Soc. Japan*, **65**, 373–390.

Nitta, Ts. and S. Sekine, 1994: Diurnal variation of convective activity over the tropical western Pacific. *J. Meteor. Soc. Japan*, **72**, 627–641.

Tanaka, M., 1992: Intraseasonal oscillation and the onset and retreat dates of the summer monsoon over East, Southeast Asia and the western Pacific region using GMS high cloud amount data. *J. Meteor. Soc. Japan*, **70**, 613–629.

北半球夏季西太平洋上における大規模対流活動の急激な季節変化

植田宏昭
(筑波大学地球科学研究科)
安成哲三
(筑波大学地球科学系)
川村隆一
(防災科学技術研究所)

西太平洋上の大規模対流活動と風の場の季節変化を、静止気象衛星の赤外黒体輻射温度 (T_{BB}) とヨーロッパ中期予報センター (ECMWF) 全球客観解析データを用いて、1980 年から 89 年の 10 年間にわたり解析した。特に、本研究では西太平洋上 20°N, 150°E 付近の大規模対流活動が、7 月下旬に急激に北上することを記載する。活発化した対流活動はそこに強い低気圧性循環を作り出し、その低気圧の南側に西風、北側に東風を引き起こす。この強い低気圧性循環は西部熱帯西太平洋上に忽然と出現する。しかし、同時期の 110°E 以西のモンスーン西風気流は加速しておらず、この急激な変化はアジアモンスーンシステムとは切り離されていることを示唆している。更に対流活発域の北側には高気圧性循環が生じ、それは日本付近の梅雨明けに対応している。また大規模対流活動の急激な北上は熱帯性低気圧活動に関連していることが明かになった。

中緯度では、7 月下旬の大規模対流活動の急激な北上前後のジオポテンシャル高度パターンから、鉛直方向に等価順圧構造になっている事が分かり、20°N, 140°E (西太平洋) 付近の対流活発域から、北方の 60°N, 180°E (ベーリング海) に向かってロスビー波が北東方向に伝播していることが示された。

この他 20°N, 150°E の海面水温 (SST) は、急激な対流活発化の約 20 日前の 7 月上旬に、29°C を越える高温に達していることを示した。この北東方向に拡大する温かい SST 領域は、7 月下旬の対流活発化と密接に関係していることが推察される。この結果より、SST の上昇は対流活動の急激な北上に対して十分条件ではないが、重要な必要条件の一つであると考えられる。